Theoretical and Applied Fracture Mechanics 124 (2023) 103736

Contents lists available at ScienceDirect

Theoretical and Applied Fracture Mechanics

journal homepage: www.elsevier.com/locate/tafmec

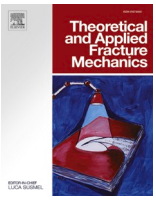

On the use of mini-CT specimens to define the Master Curve of unirradiated reactor pressure vessel steels with relatively high reference temperatures

Marcos Sánchez *, Sergio Cicero, Borja Arroyo, Ana Cimentada

LADICIM, Departamento de Ciencia e Ingeniería del Terreno y de los Materiales, University of Cantabria, Avenida de los Castros, 44, 39005 Santander, Spain

ARTICLE INFO

Keywords:
Mini-CT
Ductile-to-Brittle Transition Zone
Reference Temperature
Master Curve
RPV steels
ANP-5
A533B LUS

ABSTRACT

"Decrease if fracture toughness by thermal aging" (Therma aging(2/2)-no.2)

The safe operation of nuclear plants requires an accurate characterization of the fracture toughness of reactor pressure vessel materials, which can be reduced over time due to irradiation or thermal aging processes. This necessity is a challenge itself since the availability of specimens inside the surveillance capsules of the vessels is generally scarce. Therefore, innovative techniques have to be applied, in order to increase the reliability of fracture toughness measurements and at the same time to reduce the volume of material needed for the tests. In this paper, the Master Curve (MC) approach has been employed, combined with the use of mini-CT specimens made from two different reactor pressure vessel (RPV) steels (ANP-5 and A533B LUS). The MC methodology allows the fracture toughness of the material to be evaluated by using a single parameter: the reference temperature, T_0. This parameter has been previously estimated using mini-CT specimens in a number of unirradiated steels, most of them with relatively low T_0 values (-120 °C to −60 °C), providing satisfactory results. This paper adds further validation of the use of mini-CT specimens to define the T_0 of unirradiated RPV steels with relatively high values of this parameter. Additionally, the analysis of the fracture surfaces confirms the existence of cleavage fracture following the weakest link theory (i.e., one single initiation point), as required by the Master Curve approach.

1. Introduction

One of the main challenges when ensuring the safe operation and the life extension of nuclear power plants (NPPs) relies on the safe operation of the proper reactor pressure vessel (RPV). In this sense, a specific issue to be addressed is the embrittlement of the RPV steel due to its exposure to neutron irradiation or thermal aging processes. Traditionally, the quantification of the embrittlement level has been evaluated through Charpy impact tests of specimens introduced in certain positions of the RPV before the beginning of the plant operation, which are periodically extracted and tested. However, after the life extension of many NPPs beyond the initial lifespan, they face the problem of there being a lack of specimens to be used in the surveillance programs for long-term operation purposes. Besides, local material heterogeneities and small defects have been identified in large forgings such as those used in RPVs, which cannot be accurately addressed when using large testing specimens.

For these reasons, it is necessary to develop a methodology capable of optimizing the remaining material, which allows a direct evaluation of the fracture toughness and takes into account possible inhomogeneities of the material when required.

One of the most extended methodologies to quantify the irradiation effects in ferritic steels is the Master Curve (MC). This approach is able to provide, through a single parameter called reference temperature (T_0), a complete fracture characterization within the ductile to brittle transition zone (DBTZ) of ferritic steels. Usually, T_0 has been determined by using either standard fracture specimens, SENB or C(T), or pre-cracked Charpy specimens. However, the MC approach allows, in principle, the use of specimens with small thicknesses. This allows small scale testing techniques with miniaturized specimens to be implemented, such as miniatured compact tension specimens, also called 0.16 T C(T) or mini-CT specimens, among others. This specimen, whose typical dimensions are 10x9.6x4 mm^3, can be obtained, for instance, from an already broken half of a Charpy specimen that has been previously tested in a surveillance program. Such Charpy specimens can be subsequently reinserted into the surveillance capsule for further irradiation, and the material can then be retested at different operational stages by machining the corresponding mini-CT specimens.

Recently, the applicability of mini-CT specimens in combination

* Corresponding author.
E-mail addresses: marcos.sanchez@unican.es (M. Sánchez), ciceros@unican.es (S. Cicero), arroyob@unican.es (B. Arroyo), anaisabel.cimentada@unican.es (A. Cimentada).

https://doi.org/10.1016/j.tafmec.2022.103736
Received 23 August 2022; Received in revised form 20 December 2022; Accepted 20 December 2022
Available online 23 December 2022
0167-8442/

Table 1
Chemical composition of ANP-5 and A533B LUS steels (wt.%).

Material	C	Si	Mn	P	S	Cr	Mo	Ni	Cu
ANP-5	0.08	0.15	1.14	0.015	0.013	0.74	0.60	1.11	0.22
A533B LUS	0.24	0.41	1.52	0.028	0.023	0.08	0.49	0.43	0.19

Table 2
Material properties of ANP-5 and A533B LUS steels.

Material	σ_{ysRT} (MPa)	σ_{uRT} (MPa)	T_0 (°C)	T_{68J} (°C)	T_{41J} (°C)	RT_{NDT} (°C)	RT_{T0} (°C)
ANP-5	604	696	−38	0	−12	−28	−19
A533B LUS	460	640	+8	101	34	68	13

with the MC approach has been intensively studied on unirradiated bases [1–8] and weld [9,10] metals, as well as on irradiated materials [11–16]. However, the obtention and testing particularities of mini-CT specimens still cause concerns that must be addressed before being accepted by the different regulatory bodies and organisms. To expand the knowledge on machining, geometrical aspects, testing technology, etc., and to validate the results obtained by using mini-CT specimens in combination with the MC approach, different initiatives are being carried out, among which the European project FRACTESUS [17,18] stands out. This project provides the framework of the present research.

With all this, this paper aims to provide further validation of using mini-CT specimens to define the material Master Curve and to compare the corresponding results with those obtained using conventional fracture mechanics specimens. In this case, the analysis is focused on two unirradiated RPV steels with relatively high values of reference temperature (T_0). Thus, Section 2 presents the materials, the experimental program, and the methodology used for the application of the MC approach to mini-CT specimens; Section 3 gathers the experimental results and provides the evaluation of T_0, together with an analysis of the micromechanisms and the corresponding discussion. Finally, Section 4 presents the main conclusions.

2. Materials and methods

2.1. Materials

Two RPV steels have been used for the fracture toughness tests in mini-CT specimens: one is the ANP-5 steel, completely characterized in [19], which was taken from a weld coupon obtained by NiCrMo1 submerged arc welding wire and modified LW320/330 powder. This weld metal coupon, also known as P370 WM, emulates an RPV shell used in the first generation of German pressurized water reactors (PWRs); the second material is the A533B LUS steel, used in a round-robin organized by the Japan Society for the Promotion of Science (JSPS) and characterized in [20]. This material has a high transition temperature and a low upper shelf in unirradiated conditions, mainly due to high P and S contents. Its behavior is particularly interesting because, in unirradiated conditions, it simulates the effects of irradiation on the fracture toughness of RPV steels after a long operation. The chemical compositions are shown in Table 1.

Both materials were tested in [19] and [20] by using conventional standardized fracture specimens, obtaining the corresponding T_0 values (see Table 2). The resulting broken halves of that initial experimental campaign have been subsequently used to obtain the mini-CT specimens used in the present research.

The most relevant mechanical properties are gathered in Table 2, such as the yield stress (σ_{ysRT}) and the ultimate strength (σ_{uRT}) at room temperature, the MC reference temperature (T_0), the temperatures for energies of 68 J and 41 J measured in Charpy specimens, the reference temperature for nil-ductility transition and the reference temperature

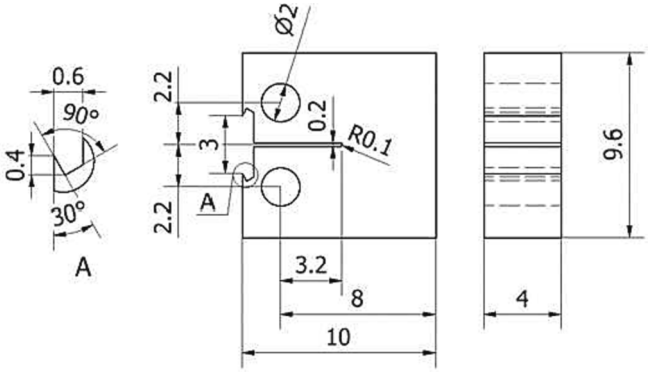

Fig. 1. The geometry of the mini-CT specimens. Dimensions in mm.

(RT_{T0}) as defined in ASME Code Cases N-629 [21] and N-631 [22]. It is worth noticing that T_0 was determined through 0.4 T SENB specimens for ANP-5 steel and compact tension (CT) specimens of different sizes (0.5 T-2 T) for the A533B LUS steel.

In this work, as the tests were carried out at different temperatures for T_0 determination, the dependence of Young's modulus and yield stress with temperature was determined according to ASTM E1921 equations (1) and (2) [23]:

$$\sigma_y\,(\mathrm{MPa}) = \sigma_{ysRT} + \frac{10^5}{(491 + 1.8T)} - 189 \tag{1}$$

$$E\,(\mathrm{GPa}) = 204 - \frac{T}{16} \tag{2}$$

2.2. Methods

2.2.1. Master Curve approach

The Master Curve (MC) is an engineering tool that enables a straightforward estimation of the fracture toughness of ferritic steels within the ductile-to-brittle transition zone (DBTZ) [24,25] and is standardized by ASTM E1921 [23]. The MC approach is based on the weakest link theory and, consequently, describes the fracture toughness results by a three parameter Weibull distribution, but only requires a single material parameter, T_0, to be defined. T_0 represents the temperature at which the median of fracture toughness, $K_{JC(med)}$, for a 1 T (25.4 mm) thick specimen is equal to 100 MPa$\sqrt{m}$. Once the corresponding T_0 is known, the MC can be defined for any probability of failure (P_f) by the following equation (3):

$$K_{JC,\,Pf} = 20 + \left[\ln\left(\frac{1}{1 - P_f}\right)\right]^{1/4} \bullet \{11 + 77 \bullet \exp[0.019 \bullet (T - T_0)]\} \tag{3}$$

Besides, when dealing with other specimen thicknesses rather than 1 T, the MC proposes a correction to convert the actual K_{JC} value into the corresponding $K_{JC(1T)}$, using the following equation (where B is the thickness of the tested specimen) (4):

$$K_{JC(1T)} = 20 + [K_{JC} - 20]\left(\frac{B}{25.4}\right)^{1/4} \tag{4}$$

This equation corrects the size (thickness) effect associated with the statistical nature of cleavage fracture: the larger the thickness the higher the possibility of finding a cleavage promoting particle along the crack

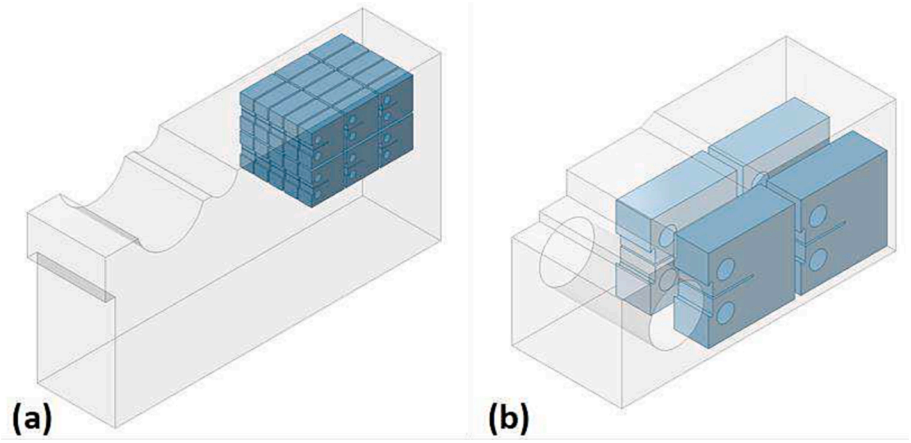

Fig. 2. Schematic of mini-CT specimen extraction for (a) ANP-5 material and (b) A533B LUS.

front.

The MC approach, therefore, makes it possible to address the three main issues of fracture characterization within the DBTZ: the scatter of the results, the dependency of fracture toughness on the temperature, and the influence of the specimen thickness. With all this, T_0 can be determined with relatively few fracture tests (6 valid tests in the best-case scenario) and a low volume of material.

2.2.2. Experimental program

The experimental campaign was conducted using 4 mm thick CT specimens (B = 4 mm). The geometry selected, shown in Fig. 1, follows the specifications of ASTM E1921 [23], thus accomplishing the general tolerance of ± 0.013 W on all dimensions (approximately ± 0.1 mm for mini-CT specimens). Additionally, a pair of knife edges were machined at the front face of the specimen to mount the crack opening displacement (COD) assuring a fixed fit to the specimen. The front face displacements were subsequently translated into the corresponding load-line displacements by applying a rotational factor of 0.73, as indicated in [23], and used for the determination of the J integral value at cleavage fracture, since its plastic part, J_p, is defined from the corresponding load-line displacement. It is noteworthy that in this work side grooves were not considered given their demonstrated little impact on this type of small specimens [26], the resulting reduced measuring capacity, and the increment of the machining cost, among other circumstances.

The mini-CT specimens were extracted from already broken fracture mechanics specimens with conventional dimensions. In the case of the ANP-5 material, 22 mini-CTs were obtained from a broken compact crack arrest specimen provided by Framatome. For the A533B LUS steel, 16 mini-CT specimens were machined from 4 halves of 2 0.5 T CT specimens provided by SCK-CEN. It is important to notice, as mentioned above, that the materials used here were employed in [19] and [20] in two previous experimental campaigns from which the corresponding T_0-values were determined. Such T_0 values, obtained from standardized specimens, will be compared to those derived in this work from mini-CT specimens. A schematic of the mini-CT specimeńs extraction is shown in Fig. 2.

The testing procedure and the subsequent analysis were performed by following the standard ASTM E1921 [23]. Before the tests, crack-like defects were introduced by fatigue pre-cracking. The length of the resulting cracks was controlled optically and also by COD measurements and the corresponding compliance (and crack length) values, ensuring a final pre-crack length within the range of 0.5 W ± 0.05 W, as specified in the ASTM E1921 [23].

Since this paper aims to characterize the fracture behavior in the DBTZ, the specimens were cooled at the selected temperature in a thermostatic chamber fed by liquid nitrogen, with electronic control in the range of ± 1 °C. In order to guarantee a homogenous temperature throughout the whole specimen material during the test, specimens were exposed to the target temperature for at least 15 min before starting the actual fracture test. Although ASTM E1921 [23] recommends attaching a thermocouple directly to the specimen, scientific literature and industrial practice accept the temperature to be monitored by a thermocouple attached to the surface of the clevis, assuming differences in the range of ± 3 °C between the clevis and specimen [4]. In the present work, for operation simplicity, this last option was chosen. The initial test temperature of each material was selected by lowering about 30–35 °C the values of T_0 shown in Table 2, as recommended in [4] with the aim of avoiding any data censoring derived from $K_{Jclimit}$ (see section 2.2.3).

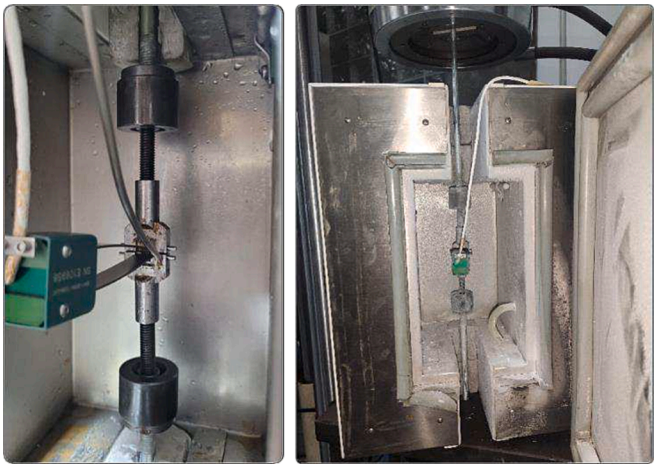

Fig. 3. Experimental setup of the mini-CT specimen.

The tests were performed in a servo hydraulic machine with a load capacity of 100 kN, subjected to a quasi-static loading rate of 1 MPa$\sqrt{m}$/s, within the range of 0.1 to 2 MPa$\sqrt{m}$/s recommended by ASTM E1921 [23]. During the tests, the load and the front face displacement (measured by means of a COD extensometer) were continuously recorded. The experimental setup is shown in Fig. 3.

From the broken halves of each specimen, the real initial crack length was determined by direct measuring according to ASTM E1921 [23], which was then used for further calculations. Additionally, the straightness of each individual crack front was checked following ASTM E1921 [23].

2.2.3. Evaluation of the reference temperature

The evaluation of the fracture toughness within the DBTZ test was

Table 3
Crack length measurements and fracture toughness test results in ANP-5.

Code	a_0 (mm)	Test temp. (°C)	$K_{JClimit}$ (MPa$\sqrt{m}$)	K_{JC} (MPa$\sqrt{m}$)	K_{JC}(1 T) (MPa$\sqrt{m}$)	δ_i
ANP-5_01	4.30	−88.3	139.27	69.75	51.32	1
ANP-5_02	4.10	−88.3	144.41	46.37	36.60	1
ANP-5_03	4.00	−77.3	143.73	69.81	51.36	1
ANP-5_05	3.98	−66.9	142.38	55.33	42.30	1
ANP-5_06	3.96	−66.9	143.48	122.79	84.75	1
ANP-5_08	4.16	−66.9	138.85	85.65	61.33	1
ANP-5_09	4.11	−66.9	140.67	55.08	42.12	1
ANP-5_10	4.17	−66.9	139.33	82.12	59.14	1
ANP-5_11	4.17	−56.1	138.04	79.04	57.24	1
ANP-5_12	4.17	−56.1	139.05	317.10	84.67[1]	0
ANP-5_13	3.98	−56.1	141.94	81.89	58.96	1
ANP-5_15	4.00	−56.1	142.74	82.92	59.64	1
ANP-5_16	4.16	−56.1	139.02	279.74	84.75[1]	0
ANP-5_17	4.01	−61.5	141.53	120.27	83.32	1
ANP-5_18	3.87	−61.5	144.35	57.32	43.49	1
ANP-5_19	4.04	−61.5	141.00	108.64	75.84	1
ANP-5_20	3.99	−61.5	141.33	56.83	43.20	1
ANP-5_21	4.03	−61.5	141.02	58.42	44.22	1
ANP-5_22	3.97	−61.5	142.86	62.18	46.40	1

[1] Censored due to large ductile crack growth and K_{JC} value exceeding $K_{Jclimit}$.

performed by calculating K_{JC}. This elastic–plastic parameter in terms of stress intensity factor units is derived from the J integral at the onset of cleavage fracture (J_c). The relationship between both parameters is the following (5):

$$K_{JC} = \sqrt{J_c \bullet \frac{E}{(1-\nu^2)}} \tag{5}$$

where E is Youngś modulus and υ is Poissońs ratio. The K_{JC} values used to define MC are valid as long as a series of criteria such as high constraint, small scale yielding, and cleavage fracture micromechanisms are addressed. In this sense, the maximum K_{JC} capacity is limited by the specimen's remaining ligament (b_0) as indicated in equation (6). The K_{JC} data that exceeds this limit must be replaced (censored) by the value of the $K_{Jclimit}$.

$$K_{JClimit} = \sqrt{\frac{E \bullet b_0 \bullet \sigma_y}{30 \bullet (1-\nu^2)}} \tag{6}$$

Equation (6) is a particular concern when using mini-CT specimens, given that their small dimensions increase the probability of censoring K_{Jc} data obtained at temperatures close to T_0 or higher.

Finally, the ductile crack growth is limited to values beyond 0.05(W-a_0) or 1 mm, the smaller of the two. When this requirement is not fulfilled, the corresponding K_{JC} value is censored by the highest uncensored K_{JC} value of the whole dataset.

Once the aforementioned two-step censoring procedure has been applied (see section 8.9.2 of ASTM E1921 [23] for further details), the next step consists of converting K_{JC} values obtained in 4 mm thick specimens (mini-CTs) into $K_{JC(1T)}$ values following equation (4).

In this work, T_0 is evaluated from the resulting $K_{JC(1T)}$ data set by using the multi-temperature method according to ASTM E1921 [23]. A provisional value of T_0, referred to as T_{0Q}, is obtained from equation (7):

$$\sum_{i=1}^{N}\delta_i \bullet \frac{\exp[0.019\bullet(T_i - T_{0Q})]}{11+77\bullet\exp[0.019\bullet(T_i - T_{0Q})]} - \sum_{i=1}^{N}\frac{(K_{JC(i)}-20)\exp[0.019\bullet(T_i - T_{0Q})]}{\{11+77\bullet\exp[0.019\bullet(T_i - T_{0Q})]\}^5} = 0 \tag{7}$$

where N is the number of specimens tested and T_i is the test temperature for the corresponding $K_{JC(i)}$ value. T_{0Q} is finally validated as T_0 if two additional conditions are met: the data included in the calculations must be tested within the temperature range of T-T_0 = ±50 °C, and (8):

$$\sum_{i=1}^{n} r_i \bullet n_i \geq 1 \tag{8}$$

where r_i is the number of uncensored data and n_i is the specimen weighting factor, see Table 5 of section 10.3 ASTM E1921 [23]). Once T_0 is determined, the relation between $K_{JC(med)}$ and T is unequivocally given by (9):

Table 4
Crack length measurements and fracture toughness test results in A533B LUS.

Code	a_0 (mm)	Test temp. (°C)	$K_{JClimit}$ (MPa$\sqrt{m}$)	K_{JC} (MPa$\sqrt{m}$)	K_{JC}(1 T) (MPa$\sqrt{m}$)	δ_i
A533B LUS_01	4.10	−30	119.03	127.79	82.58[1]	0
A533B LUS_03	3.93	−35	122.70	78.89	57.07	1
A533B LUS_04	4.31	−35	117.07	92.04	65.44	1
A533B LUS_05	4.21	−35	118.32	77.62	56.39	1
A533B LUS_06	4.37	−35	116.34	110.19	76.71	1
A533B LUS_07	4.11	−35	119.40	67.64	50.11	1
A533B LUS_08	4.05	−40	120.64	60.35	45.41	1
A533B LUS_09	4.03	−40	121.64	49.13	38.36	1
A533B LUS_10	4.05	−35	119.90	99.40	70.11	1
A533B LUS_11	4.39	−35	115.72	110.48	76.96	1
A533B LUS_12	4.03	−40	121.09	64.12	47.88	1
A533B LUS_13	4.39	−40	115.98	78.27	56.68	1
A533B LUS_14	4.39	−30	110.85	81.62	58.82	1
A533B LUS_16	4.14	−30	118.30	86.34	61.87	1

[1] Censored due to exceeding $K_{Jclimit}$.

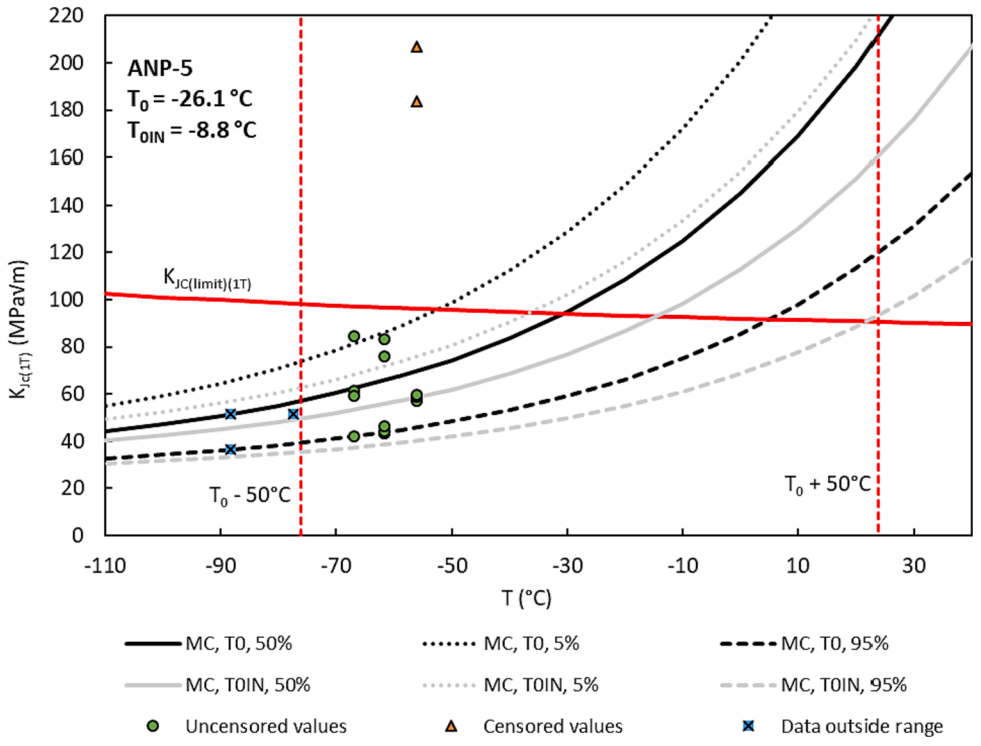

Fig. 4. Master Curve analysis of ANP-5 material.

$$K_{JC(med)} = 30 + 70 \bullet \exp[0.019 \bullet (T - T_0)] \quad (9)$$

Additionally, the K_{JC} value for any probability of failure (P_f) and working temperature (T) is given byequation (3), being the most common the curves associated with probabilities of failure of 95 %, repetitively gathered in equations (10) and (11).

$$K_{JC(0.05)} = 25.2 + 36.6 \bullet \exp[0.019 \bullet (T - T_0)] \quad (10)$$

$$K_{JC(0.95)} = 34.5 + 101.3 \bullet \exp[0.019 \bullet (T - T_0)] \quad (11)$$

Finally, the standard deviation (σ_{T0}) of the estimate of T_0 is given by (12):

$$\sigma_{T0} = \left(\frac{\beta^2}{r} + \sigma_{exp}^2\right)^{1/2} \quad (12)$$

where β is the sample size uncertainty factor determined following section 10.9.1 in ASTM E1921 [23], r is the total number of uncensored data used to calculate T_0 and σ_{exp} is the contribution of experimental uncertainties, usually taken as 4 °C.

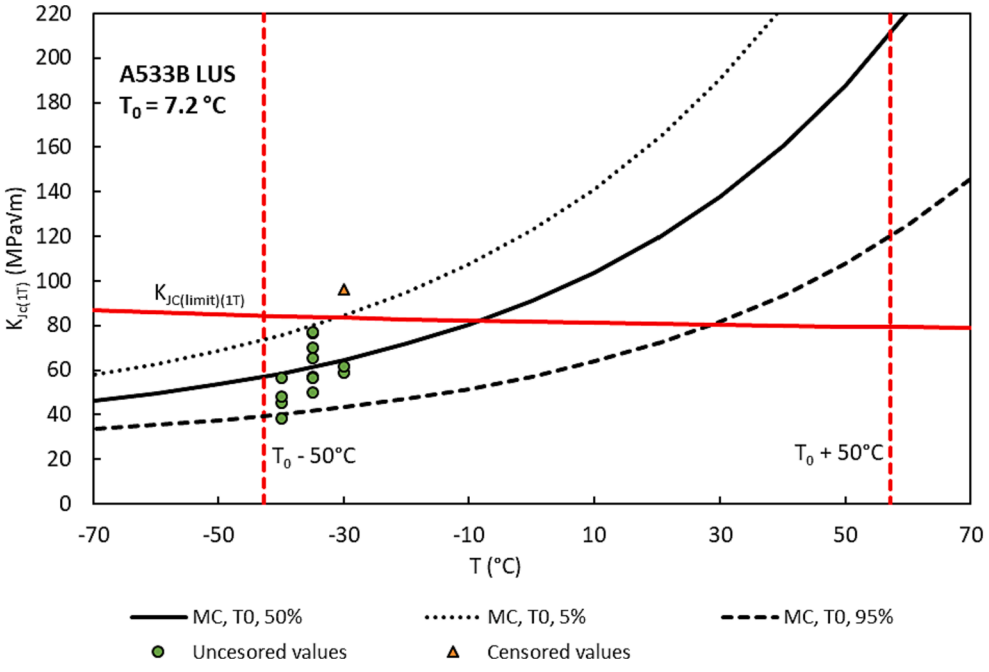

Fig. 5. Master Curve analysis of A533B LUS material.

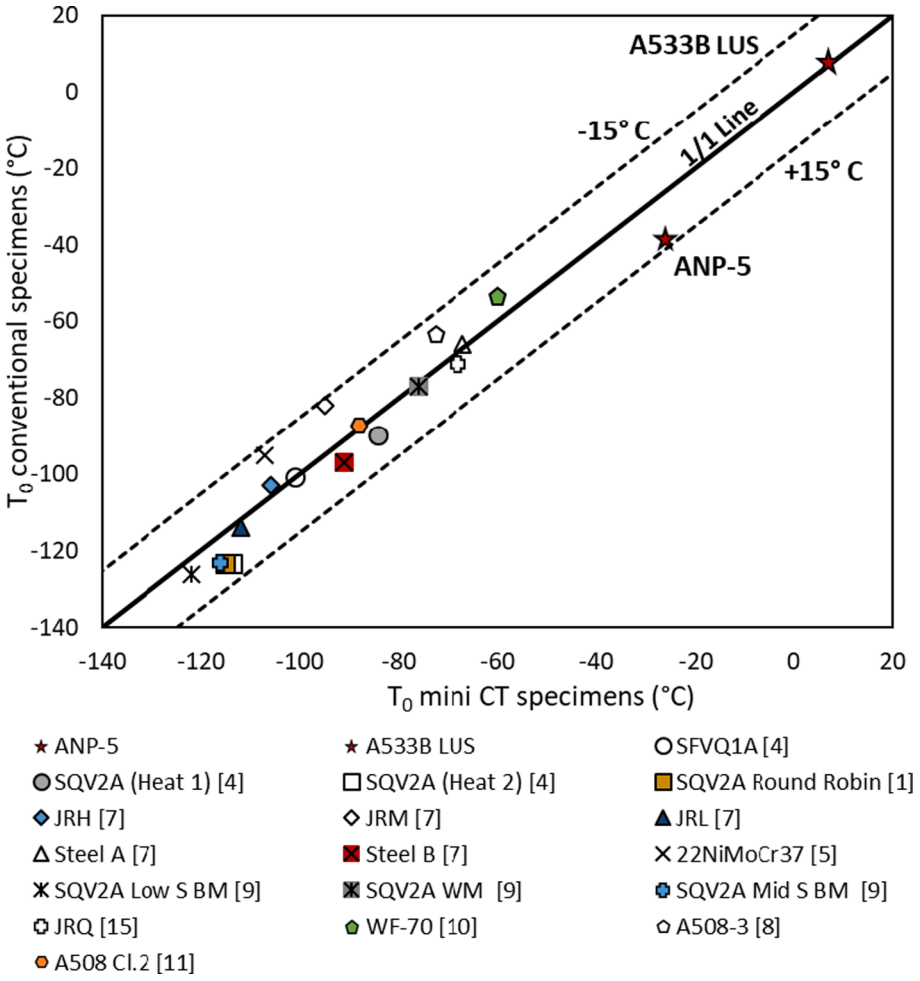

Fig. 6. Comparison between T_0 values of unirradiated materials determined from conventional specimens and T_0 values obtained using mini-CT specimens.

3. Results and discussion

3.1. Reference temperature evaluation

Table 3 and Table 4 gather the initial crack lengths, the experimental fracture toughness values, and their conversion to full-scale specimen values, together with the resulting $K_{Jclimit}$ values in steels ANP-5 and A533B LUS, respectively. It should be noted that some results were directly discarded because the crack length criterion of $a_0/W = 0.5 \pm 0.05$ was exceeded, according to ASTM E-1921 [23]. Therefore, the MC methodology was finally applied to 19 and 14 tested specimens for ANP-5 and A533B LUS respectively. All the crack fronts satisfied the straightness criterion of ASTM E1921 [23].

For the ANP-5 material, a total of two K_{JC} values were censored ($\delta_i = 0$) since they exceeded the two censoring criteria: excessive ductile crack growth (greater than $0.05 \cdot (W\text{-}a_0)$) and K_{JC} greater than $K_{Jclimit}$. These K_{JC} values were replaced as specified by ASTM E1921 [23], in this case, by the maximum uncensored K_{JC} value of the dataset. In the A533B LUS dataset, three specimens were censored because they exceeded $K_{Jclimit}$, so they were replaced by the 1 T-scaled $K_{Jclimit}$.

Fig. 4 and Fig. 5 show the MC results, including the 5 % and 95 % tolerance bounds (Eqs. (10) and (11)) together with the experimental data. Besides, the validity zone of the MC ($T_0 \pm 50$ °C) and the $K_{Jclimit(1T)}$ limit (for $b_0 = 4$ mm), have been plotted. In the case of ANP-5, three values were outside the validity range of the final T_0, which was therefore finally sustained by 16 experimental results. In the case of the A533B LUS steel all data (14) were located within the final validity range. It is evident that, for the two materials being analyzed, the MC provides a good fitting of the experimental results obtained through mini-CT specimens.

Furthermore, it can be observed that the validity zone (area below the censoring line and within $T_0 \pm 50$ °C) of the results obtained in mini-CT specimens is quite reduced. Since the remaining ligament is proportional to the thickness of the specimen, decreasing the thickness implies lower values of $K_{Jclimit}$. These particularities make it necessary to test well below the T_0 (e.g., $T_0 - 30$ °C) to obtain sufficient uncensored values, taking care not to violate the above referred temperature range required for T_0 analysis.

With all this, T_0 valid values of −26.1 °C ± 6.7 °C and 7.2 °C ± 6.9 °C were determined for ANP-5 and A533B LUS steels respectively. In comparison with the T_0 values obtained from large specimens (shown in Table 2 and equal to −38 °C and + 8 °C for ANP-5 and A533B LUS respectively), ANP-5 presented a higher T_0 with a difference of + 11.9 °C, while A533B LUS showed a lower T_0, with a deviation of −0.8 °C. In addition, the homogeneity of the materials was verified with the screening procedure provided by ASTM E1921 standard, Section 10.6.2 [23]. The results, obtained by using T0TEM software [27], reveal that ANP-5 material does not meet the screening criterion, see equation (13), (i.e., it is an inhomogeneous material) meanwhile A533B LUS material does meet the criterion (homogeneous material). Thus, for ANP-5 material, Appendix X.5, Section X.5.2 (Simplified Method) has been applied with the aim of obtaining a conservative estimate of the reference temperature in non-homogeneous materials (T_{0IN}), which resulted −8.8 °C. In this particular case, T_{0IN} coincides with T_{0scrn}, as defined by [23].

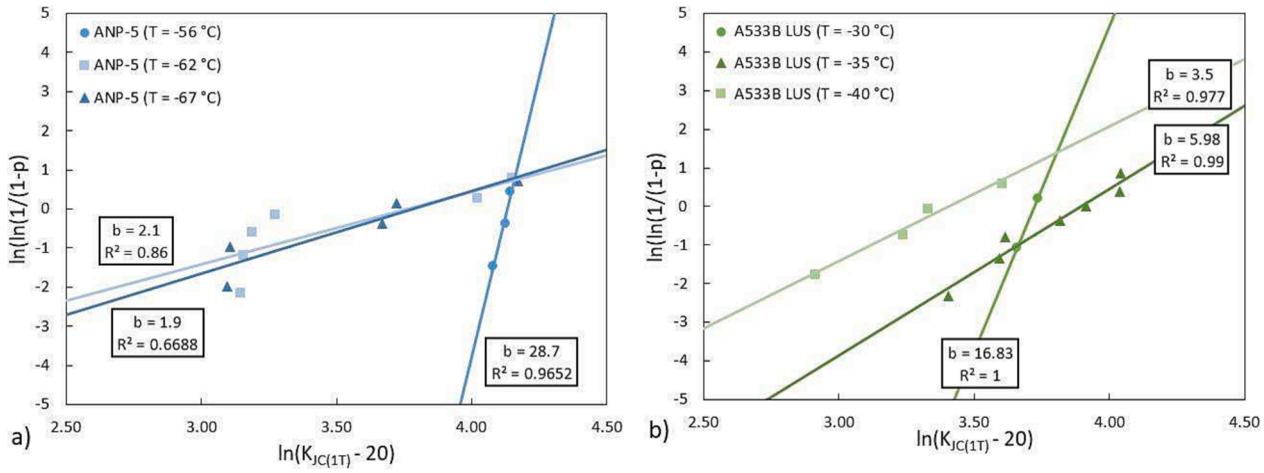

Fig. 7. Weibull plot for valid data of steels: a) ANP-5 and b) A533B LUS.

$$T_{0scm} - T_0 \leq 1.44\sqrt{\frac{\beta^2}{r}} \tag{13}$$

The obtained value of T_{0IN} should be used in subsequent structural integrity assessments and reporting, the corresponding Master Curve being also shown in Fig. 4. However, as long as the purpose of this paper is to verify the suitability of mini-CT specimen to characterize the DBTZ, and also that the reference temperature of the ANP-5 material obtained from conventional specimens (see [19,28]) was T_0 as defined by the standard procedure of [23], not by Appendix X5 (i.e., in [19,28] the material resulted homogeneous), the value of the reference temperature obtained here through mini-CT specimens and used for the mentioned verification is −26.1 °C, and not −8.8 °C.

For a better understanding of the capacity of mini-CT specimens to determine the material T_0 and, thus, the corresponding MC, a review of the literature was conducted. The efforts were focused on unirradiated materials (both base metal and weld metal), as is the case in the two steels analyzed in this work. Fig. 6 shows a comparison of the T_0 values obtained with large conventional specimens with those obtained using mini-CT specimens. All the values, including the materials tested in the present work, are located between the bands of ± 15 °C, as shown in the graph. Thus, in general, the values of T_0 obtained with mini-CT specimens are in good agreement with those obtained with larger specimens. Here it is interesting to point out the that published data (and the results of this paper) show an interesting behavior: sometimes, the use of mini-CT specimens provides values of T_0 that are lower than those obtained from conventional fracture specimens, while in other occasions mini-CT specimens generate higher values of T_0. Considering the data found in the literature, the T_0 values calculated in this study seem to be highly consistent, something which is particularly relevant if it is considered that the T_0 values analyzed in the literature are basically between −120 °C and −60 °C, whereas the values reported in this work provide validation of the use of mini-CT specimens in a well-above temperature range, extending their validation to define T_0 (and the MC).

3.2. Additional evidences on the validity of mini-CT specimens

The use of mini-CT specimens in surveillance programs still presents concerns from regulatory bodies, who require further evidences about the reliability of this technique. Beyond the sound results gathered in Fig. 6, this section will provide additional reasoning supporting the use of mini-CTs to define the MC of RPV steels. This reasoning is focused on two main aspects directly related to the definition of the MC: the value of the shape parameter (b) of the Weibull distribution and the fulfillment of the weakest link theory in mini-CT specimens.

Concerning the shape parameter, the MC assumes that fracture is controlled by weakest link statistics and follows a three parameter Weibull distribution. Accordingly, within the scope of small-scale yielding conditions, the cumulative failure probability (P_f) on which the MC is based follows equation (14):

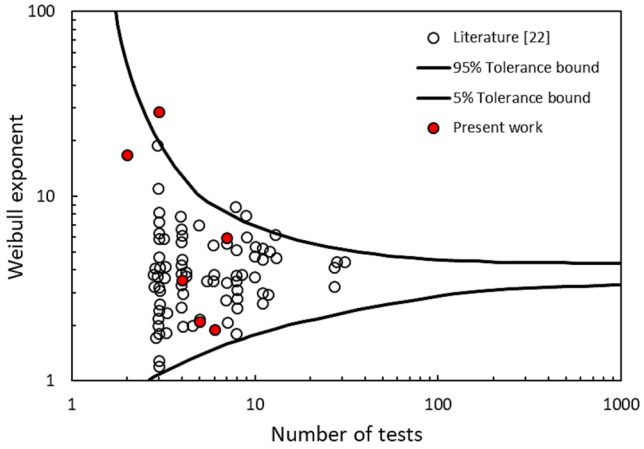

Fig. 8. Weibull exponent (shape parameter, b) vs the number of specimens, and confidence bands.

$$P_f = 1 - e^{-\frac{B}{B_0}\bullet\left(\frac{K_{JC}-K_{min}}{K_0-K_{min}}\right)^b} \tag{14}$$

where K_{JC} is the fracture toughness for the selected probability of failure (P_f), B is the specimen thickness and B_0 is the reference specimen thickness assumed in this methodology (B_0 = 25.4 mm, also referred to as 1 T). The three Weibull parameters are: K_0, the scale parameter located at the 63.2 % cumulative failure probability level; K_{min}, the location parameter, representing the value of the stress intensity factor below which cleavage does not occur, and; b, the shape parameter. Both K_{min} and b take the same values for all ferritic steels and have been amply justified in conventional specimens, providing values of 20 MPa$\sqrt{m}$ and 4, respectively [24,25,29,30].

With the aim of providing additional support to the use of shape parameter of 4, as proposed by the ASTM E1921 [23] based on [25], in mini-CT specimens, Fig. 7 shows the Weibull plot for uncensored data of the ANP-5 and the A533B LUS steels, assuming a K_{min} equal to 20 MPa$\sqrt{m}$. The K_{JC} values are rank ordered and assigned an estimate of the median rank probability (p) [1], which is given by (15):

$$p = \frac{(i - 0.3)}{N + 0.4} \tag{15}$$

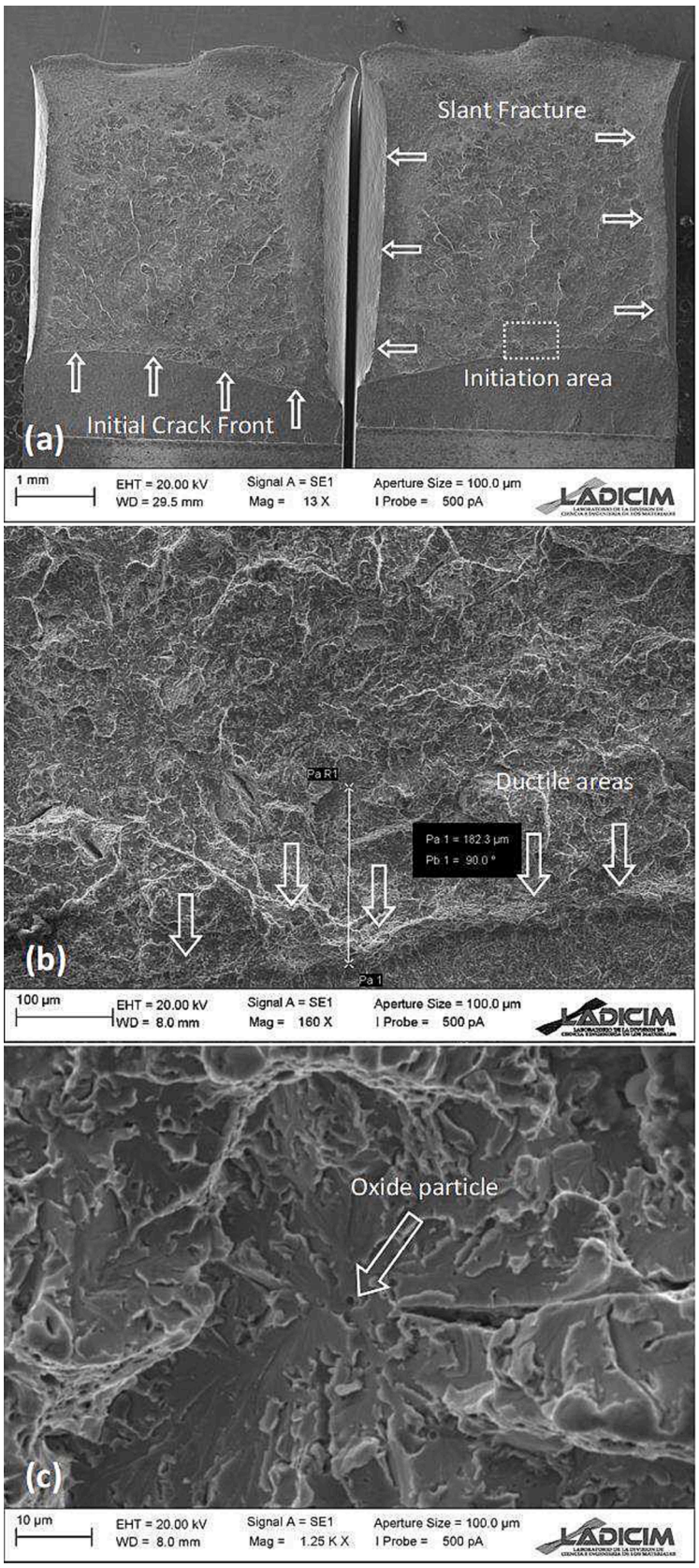

Fig. 9. SEM image of the fracture surface of ANP-5_13 specimen, with three different magnifications. (a) general view of the two broken halves; (b) detail of the crack front; (c) detail of the initiation point.

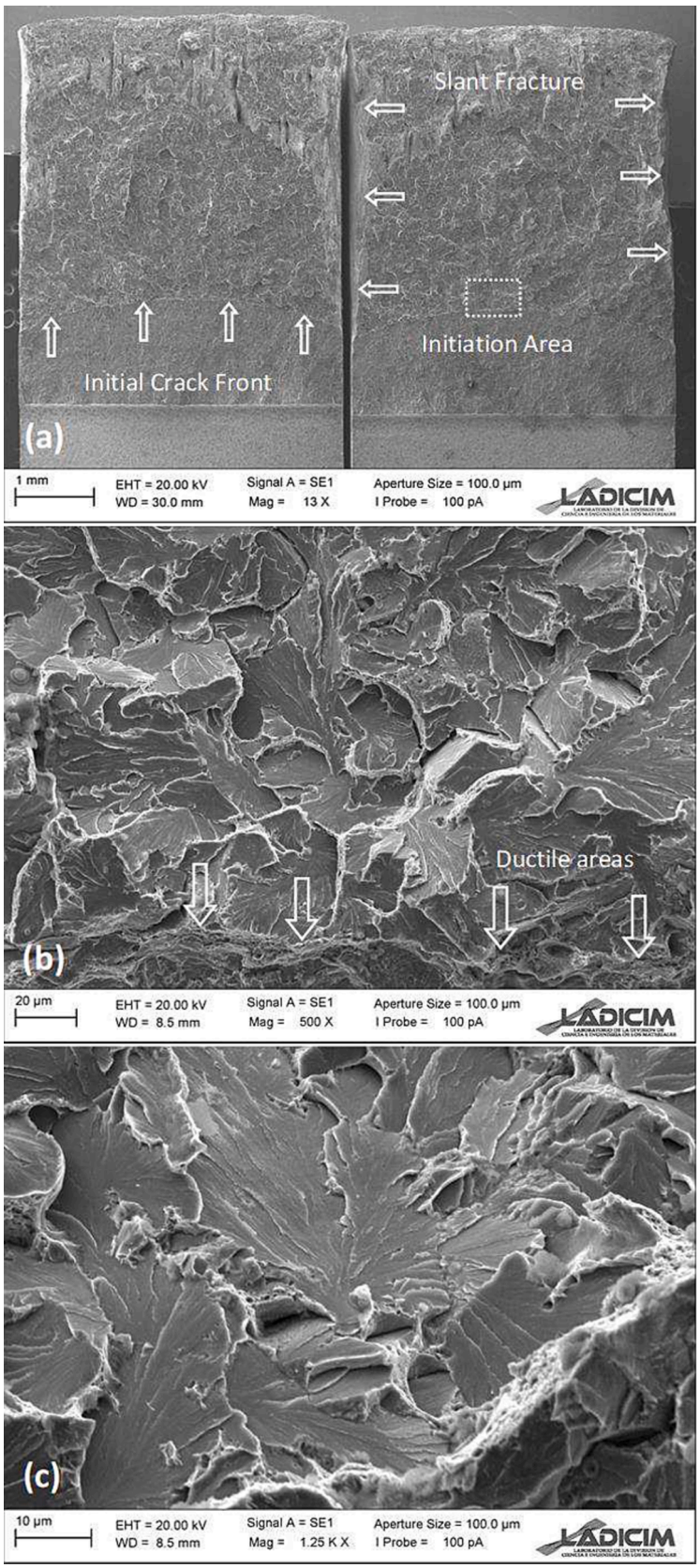

Fig. 10. SEM image of the fracture surface of A533B LUS_13 specimen, with three different magnifications. (a) general view of the two broken halves; (b) detail of the crack front; (c) detail of the initiation point.

where i is the rank of the K_{JC} value and N is the total number of K_{JC} values. The Weibull exponents (i.e., the slopes of the fitting lines) range between 1.9 and 28.7. Fig. 8 shows these fitted Weibull exponents in relation to the number of tests, together with a number of data from the literature that were used to define b in conventional specimens [25]. It can be observed how the results of the present study generally fall within the 5 % and 95 % tolerance accepted by the literature (5 out of 6 results). There are two slopes that are clearly higher than the others, but here it is important to note the fact that they have been obtained with only two and three points, respectively, in ANP-5 (-56 °C) and A533 LUS (-30 °C) steels. Overall, the use of 4 as the shape parameter in mini-CT specimens seems a reasonable practice based on the evidence found here.

Concerning the fulfillment of the weakest link statistics, which is the base to use the three parameter Weibull distribution, this requires the fracture process to be caused by cleavage (brittle micromechanism) with a single initiation point. Multiple initiation points would also imply brittle processes, but not following the weakest link theory (this is the case of fracture processes within the material Lower Shelf). Therefore, the aim here is to verify whether the mini-CT specimens tested in the experimental program failed by cleavage fracture or not, and also if there was a single (main) initiation site. In this sense, the fracture surfaces of all tested specimens were examined with a scanning electron microscope (SEM).

Fig. 9 and Fig. 10 show, as an example, the fracture surfaces observed in one specimen of each material under different magnifications, focusing on the most likely initiation zone. In both cases, the majority of the fracture surfaces begin with very narrow (a few microns) ductile areas along the initial crack front (see Fig. 9a and 10a), where micro-voids are present as can be seen in Fig. 9b and 10b. After this limited ductile tearing, the predominant failure micromechanism was cleavage fracture in all cases. It was not unusual though to find small areas of ductile fracture. Additionally, a small area of slant fracture was observed at the sides of the specimens, as a result of the plane stress effect in that region (see Fig. 9a and 10a).

In addition, there was a single initiation point in all cases, or a clearly main initiation point (see Fig. 9a and 10a), which tended to be found close to the middle of the specimen, where triaxiality conditions are maximum. Fig. 9c shows a detail of the initiation site, where an oxide was identified as the triggering particle of cleavage. Fig. 10c presents the most likely initiation point, although no particle was found in this case.

The SEM analysis demonstrates thus that the fracture processes in the mini-CT specimens analyzed in this work have followed the weakest link theory, with cleavage fracture governing the fracture and with a single initiation point triggering the whole process.

4. Conclusions

This paper analyzes and validates the use of mini-CT specimens to define the Master Curve (MC) of two different unirradiated RPV steels, ANP-5 and A533B LUS. With this aim, the reference temperature (T_0) has been determined using mini-CT specimens, and the fracture micromechanisms were evaluated by SEM analysis. The main conclusions are:

- The T_0 values of the two materials were successfully obtained from the fracture toughness tests performed on mini-CT specimens. The obtained values (-26.1 °C for ANP-5 and + 7.2 °C for A533B LUS) are consistent with those obtained from standard specimens (-38 °C and + 8 °C, respectively).
- The results provide further evidence of the reliability of using mini-CT specimens to define T_0. Besides, this new evidence is provided in two unirradiated steels with T_0 values well above the validation range found in the literature.
- With all the results put together, the differences between the values of T_0 obtained using mini-CT specimens and those obtained using conventional specimens are generally within ± 15 %.
- The analysis of the fracture micromechanisms and the Weibull shape parameter provides additional evidence about the fulfillment of two MC assumptions when working with mini-CT specimens: the fracture process follows weakest link statistics and the shape parameter can be assumed to take a value of 4.

CRediT authorship contribution statement

Marcos Sánchez: Conceptualization, Investigation, Methodology, Data curation, Writing – original draft. **Sergio Cicero:** Conceptualization, Investigation, Methodology, Funding acquisition, Writing – review & editing. **Borja Arroyo:** Investigation, Data curation, Writing – review & editing. **Ana Cimentada:** Investigation, Data curation.

Declaration of Competing Interest

The authors declare that they have no known competing financial interests or personal relationships that could have appeared to influence the work reported in this paper.

Data availability

Individual data for the fracture tests found in this document may be found in https://www.openaire.eu/.

Acknowledgments

This research has received funding from the Euratom research and training programme 2019-2020 under grant agreement N° 900014.

The authors are deeply grateful to all the consortium members of the FRACTESUS project. The authors also wish to dedicate this work to the memory of Dr. Tomasz Brynk, FRACTESUS project coordinator and outstanding colleague.

References

[1] M. Yamamoto, A. Kimura, K. Onizawa, K. Yoshimoto, T. Ogawa, Y. Mabuchi, et al., A round Robin program of master curve evaluation using miniature C(T) specimens-3RD report: Comparison of T0 under various selections of temperature conditions, Am Soc Mech Eng Press Vessel Pip Div PVP 1 (2014) 1–7, https://doi.org/10.1115/PVP201428898.

[2] Yamamoto M, Onizawa K, Yoshimoto K, Ogawa T, Mabuchi Y, Miura N. A Round Robin Program of Master Curve Evaluation Using Miniature C(T) Specimens — 2nd Report: Fracture Toughness Comparison in Specified Loading Rate Condition. Vol. 1B Codes Stand., vol. 1 B, American Society of Mechanical Engineers; 2013, p. 1–8. 10.1115/PVP2013-97936.

[3] M. Yamamoto, A. Kimura, K. Onizawa, K. Yoshimoto, T. Ogawa, A. Chiba, et al., A round robin program of Master Curve evaluation using miniature C(T) specimens: First round robin test on uniform specimens of reactor pressure vessel material, Am Soc Mech Eng Press Vessel Pip Div PVP 6 (2012) 73–79, https://doi.org/10.1115/PVP2012-78661.

[4] Miura N, Soneda N. Evaluation of Fracture Toughness by Master Curve Approach Using Miniature C(T) Specimens. ASME 2010 Press. Vessel. Pip. Conf. Vol. 1, vol. 77, ASMEDC; 2010, p. 593–602. 10.1115/PVP2010-25862.

[5] R. Chaouadi, E. Van Walle, M. Scibetta, R. Gérard, On the use of miniaturized ct specimens for fracture toughness characterization of RPV materials, Am Soc Mech Eng Press Vessel Pip Div PVP 1B–2016 (2016) 1–10, https://doi.org/10.1115/PVP2016-63607.

[6] Y. Ha, T. Tobita, H. Takamizawa, Y. Nishiyama, Fracture toughness evaluation of neutron-irradiated reactor pressure vessel steel using miniature-C(T) specimens, Am Soc Mech Eng Press Vessel Pip Div PVP 1A–2017 (2017) 1–5, https://doi.org/10.1115/PVP2017-65568.

[7] T. Tobita, Y. Nishiyama, T. Ohtsu, M. Udagawa, J. Katsuyama, K. Onizawa, Fracture Toughness Evaluation of Reactor Pressure Vessel Steels by Master Curve Method Using Miniature Compact Tension Specimens, J Press Vessel Technol 137 (2015) 4–11, https://doi.org/10.1115/1.4029428.

[8] Z. Zhou, Z. Tong, G. Qian, F. Berto, Specimen size effect on the ductile-brittle transition reference temperature of A508–3 steel, Theor Appl Fract Mech 104 (2019), 102370, https://doi.org/10.1016/j.tafmec.2019.102370.

[9] M. Yamamoto, N. Miura, Applicability of miniature-c(T) specimen for the master curve evaluation of rpv weld metal and heat affected zone, Am Soc Mech Eng Press Vessel Pip Div PVP (2016) 1B–2016, https://doi.org/10.1115/PVP2016-63762.

[10] M.A. Sokolov, Use of mini-CT specimens for fracture toughness characterization of low upper-shelf linde 80 weld before and after irradiation1, Am Soc Mech Eng

Press Vessel Pip Div PVP 1A–2018 (2018) 1–6, https://doi.org/10.1115/PVP201884804.
[11] Uytdenhouwen I, Chaouadi R. Effect of neutron irradiation on the mechanical properties of an a508 cl.2 forging irradiated in a bami capsule. Am Soc Mech Eng Press Vessel Pip Div PVP 2020;1:2–10. 10.1115/PVP2020-21513.
[12] Server W, Sokolov M, Yamamoto M, Carter R. Inter-Laboratory Results and Analyses of Mini-C(T) Specimen Testing of an Irradiated Linde 80 Weld Metal. Vol 1A Codes Stand 2018. 10.1115/PVP2018-84950.
[13] Y. Ha, T. Tobita, T. Ohtsu, H. Takamizawa, Y. Nishiyama, Applicability of Miniature Compact Tension Specimens for Fracture Toughness Evaluation of Highly Neutron Irradiated Reactor Pressure Vessel Steels, J Press Vessel Technol 140 (2018) 1–6, https://doi.org/10.1115/1.4040642.
[14] T. Sugihara, T. Hirota, H. Sakamoto, K. Yoshimoto, K. Tsutsumi, T. Murakami, Applicability of miniature C(T) specimen to fracture toughness evaluation for the irradiated japanese reactor pressure vessel steel, Am Soc Mech Eng Press Vessel Pip Div PVP 1A–2017 (2017) 1–8, https://doi.org/10.1115/PVP2017-66206.
[15] Yamamoto M. The Master Curve Fracture Toughness Evaluation of Irradiated Plate Material JRQ Using Miniature-C(T) Specimens. Vol. 1A Codes Stand., vol. 1A-2017, American Society of Mechanical Engineers; 2017, p. 1–8. 10.1115/PVP2017-66085.
[16] M. Lambrecht, R. Chaouadi, I. Uytdenhouwen, R. Gérard, Fracture toughness characterization in the transition and ductile regime of an a508 type weld metal with the mini-ct geometry before and after irradiation, Am Soc Mech Eng Press Vessel Pip Div PVP 1 (2020) 1–7, https://doi.org/10.1115/PVP2020-21515.
[17] Brynk T, Lambrecht M, Uytdenhouwen I, Arffman P, Altstadt E, Petit T. FRACTESUS Project: General Framework of Materials Selection and Testing Processes. Vol. 4 Mater. Fabr., American Society of Mechanical Engineers; 2021. 10.1115/PVP2021-61906.
[18] S. Cicero, M. Lambrecht, H. Swan, P. Arffman, E. Altstadt, T. Petit, et al., Fracture mechanics testing of irradiated RPV steels by means of sub-sized specimens: FRACTESUS project, Procedia Struct Integr 28 (2020) 61–66, https://doi.org/10.1016/j.prostr.2020.10.008.
[19] Hein H, Keim E, Schnabel H, Seibert T, Gundermann A. Final results from the crack initiation and arrest of irradiated steel materials project on fracture mechanical assessments of pre-irradiated RPV steels used in German PWR. ASTM Spec Tech Publ 2010;1513 STP:40–63. 10.1520/stp49002s.
[20] R. Chaouadi, M. Scibetta, E. Van Walle, R. Gérard, On the use of the Master Curve based on the precracked Charpy specimen, Am Soc Mech Eng Press Vessel Pip Div PVP 393 (1999) 35–46.
[21] ASME Boiler and Pressure Vessel Code–Code Case N-629. Use of Fracture Toughness Test Data to Establish Reference Temperature for Pressure Retaining Materials 1991;Section XI.
[22] ASME Boiler and Pressure Vessel Code–Code Case N-631. Use of Fracture Toughness Test Data to Establish Reference Temperature for Pressure Retaining Materials Other Than Bolting for Class 1 Vessels 1999;Section II.
[23] ASTM E1921. Standard Test Method for Determination of Reference Temperature, T0, for Ferritic Steels in the Transition Range. West Conshohocken, PA: ASTM International; 2021. 10.1520/E1921-21.
[24] K. Wallin, Master curve analysis of the "Euro" fracture toughness dataset, Eng Fract Mech 69 (2002) 451–481, https://doi.org/10.1016/S0013-7944(01)00071-6.
[25] K. Wallin, The scatter in KIC-results, Eng Fract Mech 19 (1984) 1085–1093, https://doi.org/10.1016/0013-7944(84)90153-X.
[26] Wallin K, Yamamoto M, Ehrnstén U. Location of Initiation Sites in Fracture Toughness Testing Specimens: The Effect of Size and Side Grooves. Vol. 1B Codes Stand., vol. 1B-2016, American Society of Mechanical Engineers; 2016. 10.1115/PVP2016-63078.
[27] Shelton L, Bosley C. T0TEM T0 Test Evaluation Module. Https://SoftwareNasaGov/Software/MFS-33829-1 2021.
[28] Brynk T, Uytdenhouwen I, Arffman P, Altstadt E, Kopriva R, Obermeier F, et al. FRACTESUS Project: Final Selection of RPV Materials for Unirradiated and Irradiated Round Robins. Vol. 1 Codes Stand., American Society of Mechanical Engineers; 2022, p. 1–11. 10.1115/PVP2022-83871.
[29] K. Wallin, T. Saario, K. Törrönen, Statistical model for carbide induced brittle fracture in steel, Met Sci 18 (1984) 13–16, https://doi.org/10.1179/030634584790420384.
[30] K. Wallin, The size effect in KICresults, Eng Fract Mech 22 (1985) 149–163, https://doi.org/10.1016/0013-7944(85)90167-5.